Available online at www.sciencedirect.com
ScienceDirect
Ceramics International 37 (2011) 3095–3099
CERAMICS INTERNATIONAL
www.elsevier.com/locate/ceramint

Thermal diffusivity of three-dimensional needled C/SiC–TaC composites

Jie Chen, Yiguang Wang *, Laifei Cheng, Litong Zhang

National Key Laboratory of Thermostructure Composite Materials, Northwestern Polytechnical University, Xi'an Shanxi 710072, PR China

Received 4 May 2011; received in revised form 11 May 2011; accepted 11 May 2011
Available online 17 May 2011

Abstract

Three-dimensional needled carbon fiber reinforced SiC–TaC composites were prepared by combination of slurry infiltration and reactive melt infiltration. The thermal diffusivity of the composites with different TaC contents was characterized in the temperature range from room temperature to 1400 °C. The results revealed that the temperature dependent thermal diffusivity behavior was independent on TaC content, while the thermal diffusivity values of the composites were influenced by their microstructures. A model based on lattice vibration and microstructure was used to discuss the thermal diffusivity behavior of the C/SiC–TaC composites.

Keywords: Thermal diffusivity; C/SiC–TaC composites; Microstructure; Reactive melt infiltration

1. Introduction

Carbon fiber reinforced silicon carbide (C/SiC) composites have been widely applied for thermal protection system (TPS) of aerospace vehicles due to their excellent thermomechanical properties and oxidation resistance [1–3]. With the development of hypersonic vehicles, the TPS requires C/SiC to withstand ultrahigh temperatures [4,5]. One approach to improve the temperature tolerance of C/SiC is by adding refractory carbides or borides into them [6–14]. TaC modified C/SiC (C/SiC–TaC), showing good properties at ultrahigh temperatures [6], has potential applications for TPS of hypersonic vehicles.

Thermal diffusivity is one of the most important properties for TPS applications. In the past years, several studies have been carried out on the thermal diffusivity behavior of the C/SiC composites. Tawil et al. [15] studied the effect of density on thermal diffusivity properties of C/SiC. They found that the value of thermal diffusivity increased with increasing density at all directions. Yamada et al. [16,17] analyzed the thermal conductivities of SiC/SiC composites. The results indicated that CVI-SiC/SiC had a higher thermal diffusivity than PIP-SiC/SiC, and that the thermal diffusivity of CVI-SiC/SiC decreased with the increase in the fiber volume fraction. Suresh Kumar [18] studied the effect of siliconization conditions on the thermal diffusivity of 3D needled C/SiC composites. Although many data have been reported in literatures on the thermal diffusivity of C/SiC, there is little report about refractory carbides or borides modified C/SiC composites. In this paper, we studied the thermal diffusivities of the 3D needled C/SiC–TaC composites. The effect of microstructure and composition of C/SiC–TaC on their thermal diffusivities was investigated. The mechanism of thermal diffusivity for the C/SiC–TaC was discussed. Such understanding of thermal diffusivity for the C/SiC–TaC is helpful for applying this composite to TPS of hypersonic vehicles.

2. Experimental procedure

3D needled felt was fabricated by a needle-punching technique with alternatively stacked 0° weftless piles (T-300^{TM}, HTA-1000, TOHO, Japan), short-cut-fiber webs, and 90° weftless piles. The fiber volume fraction was about 35%. TaC powders (99.5% purity, ~1 μm, Ningxia Orient Tantalum Industry, China) with dispersant solution were ball milled 12 h to form slurry. The slurry was then infiltrated into the needled felt under a pressure of 0.4–0.5 MPa in a lab-made impregnation set up. The impregnation time was about 30 min. The

* Corresponding author at: National Key Laboratory of Thermostructure Composite Materials, Northwestern Polytechnical University, P.O. Box 547, 127# You-Yi West Road, Xi'an Shanxi 710072, PR China.
Tel.: +86 29 88494914; fax: +86 29 884920.
E-mail address: wangyiguang@nwpu.edu.cn (Y. Wang).

0272-8842/$36.00
doi:10.1016/j.ceramint.2011.05.046

different TaC content in the felt was controlled by the amount of slurry. Three kinds of preforms were obtained with the TaC content of 4.5 vol%, 7 vol%, and 10.7 vol%, respectively. Carbon was introduced into the preforms as matrix by chemical vapor infiltration (CVI) using natural gas as precursor in the temperature range of 1050–1100 °C. Molten silicon was then infiltrated into the carbon matrix to form silicon carbide at the temperature of 1450–1650 °C for 1–3 h. As comparison, C/SiC without TaC addition was prepared in the same process. The samples with TaC content of 4.5 vol%, 7 vol%, and 10.7 vol% were labeled as C/SiC–TaC-4, C/SiC–TaC-7, and C/SiC–TaC-10 respectively.

The thermal diffusivity of the samples was measured by using laser flash apparatus (LFA427, NETZSCH Company, Germany). The size of specimens was Φ12.7 mm × 2 mm. All measurements were conducted in an argon atmosphere from room temperature to 1400 °C. In these tests, the specimens were subjected to a short duration thermal pulse. The energy of the pulse absorbed at the front face, resulting in the temperature rise in the rear face. The temperature rise was collected by a collecting system. Thermal diffusivity was calculated from the specimen thickness and the time ($t_{1/2}$) for the rear face temperature to reach half of its maximum value. For each specimen, thermal diffusivity was measured ($\alpha = 0.1388\ L^2/t_{1/2}$) three times at each temperature point.

The phases of the composites were analyzed by X-ray diffraction (XRD, Rigaku-D/max-2400, Tokyo, Japan) with Cu Kα radiation. The matrix-flushing method [19] was used by XRD for qualitative analysis of the phases. Alumina as an internal reference material was used in these tests. The open porosities and bulk densities of the samples were measured by Archimedes' method. The microstructure of the specimens was observed by scanning electron microscope (SEM, JEOL 6700F, Tokyo, Japan).

3. Results and discussion

Fig. 1 shows the XRD patterns of the composites. It is seen that the C/SiC–TaC composites consist of SiC, TaC, carbon and

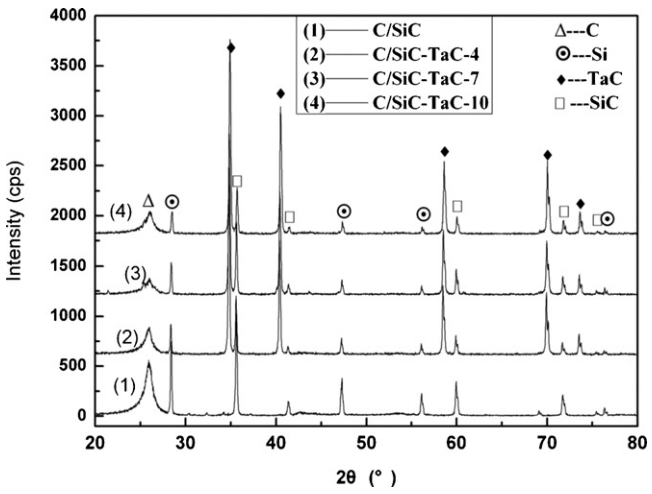

Fig. 1. XRD patterns of C/SiC and 3D needled C/SiC–TaC composites.

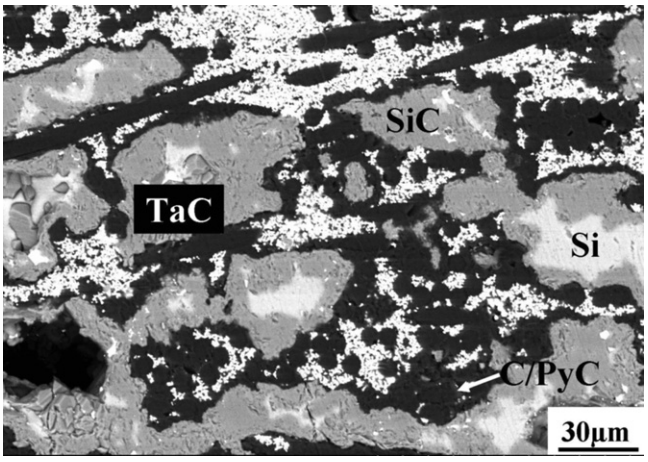

Fig. 2. A typical backscattering image of C/SiC–TaC composite.

residual Si. Carbon phase includes the un-reacted carbon matrix and carbon fibers. Residual silicon exists in the materials due to the RMI process [20]. There is no tantalum silicides observed from the patterns, indicating that the TaC did not react with Si during the RMI process. The backscattering image of C/SiC–TaC composites (Fig. 2) clearly shows the distribution of each component: Carbon fiber and pyrolytic carbon (C/PyC) substructure with TaC dispersion, the formed SiC matrix, and the residual silicon. The density and open porosity of the composites are given in Table 1. The composites with more TaC have higher density. C/SiC–TaC-7 has the least open porosity among the four composites.

The thermal diffusivity of the composites as a function of temperature is shown in Fig. 3. As can be seen, the temperature dependent thermal diffusivity of the C/SiC–TaC composites is similar to that of the C/SiC composites: the thermal diffusivity decreases continuously as increasing temperature and there is a transition point at 1200 °C beyond which the decrease rate of thermal diffusivity becomes larger. Obviously, the addition of TaC into C/SiC does not change the tendency of temperature dependent thermal diffusivity but its values. C/SiC–TaC has smaller values of thermal diffusivity than C/SiC. However, the thermal diffusivity does not monotonically decrease with the increase in the TaC content: C/SiC–TaC-4 has the smallest value, while the C/SiC–TaC-7 has the value close to that of C/SiC and the C/SiC–TaC-10 has the value between them. It indicates that other factors like the open porosities can also affect the value of thermal diffusivity.

The thermal diffusivity of solid materials depends on their lattice vibration and microstructure. The temperature dependent thermal diffusivity can be expressed by the following

Table 1
Porosities and densities of the composites.

Samples	C/SiC	C/SiC–TaC-4	C/SiC–TaC-7	C/SiC–TaC-10
Open porosity(%)	9.29	10.72	7.81	9.68
Density (g/cm^3)	1.93	2.28	2.52	2.62
Si (wt%)	13.08	6.63	7.11	7.56
SiC (wt%)	24.86	19.46	26.81	22.58

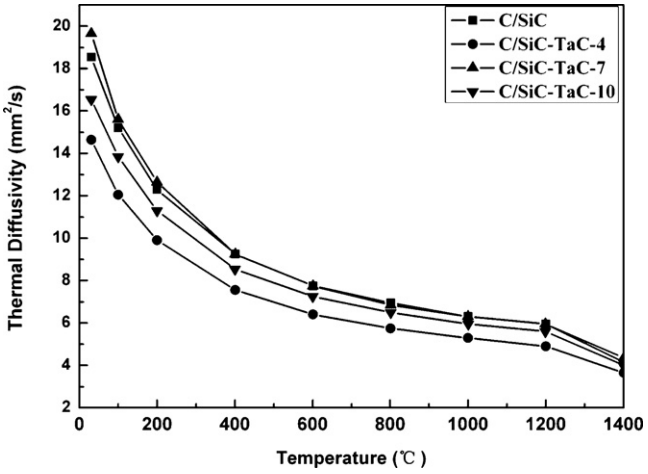

Fig. 3. Thermal diffusivity of the composites as a function of temperature.

equation [21]:

$$\frac{1}{\alpha} = AT + B \tag{1}$$

where α is the thermal diffusivity, A and B are constants.

The data of thermal diffusivity before 1200 °C (Fig. 3) were fitted by equation 1. The obtained values of A and B were listed in Table 2. As can be seen, the A values of all the composites are close to each other while the B value of C/SiC and C/SiC–TaC-7 are close and much lower than the values of the other two composites.

The thermal conductivity can be described as the following equation [22]:

$$\lambda = \frac{1}{3} cvl \tag{2}$$

where λ is the thermal conductivity, ν the average phonon velocity, c the heat capacity, l the mean free path of phonon. ν is generally considered as a constant because it is almost temperature independent [21]. The relationship between thermal conductivity (λ) and thermal diffusivity (α) is $\alpha = \lambda/\rho c$ [23], where ρ is the density. Therefore, α is proportional to the phonon's mean free path l. The value of l is composed of three aspects [21,24]:

$$\frac{1}{l_{tot}} = \frac{1}{l_{pp}} + \frac{1}{l_{pd}} + \frac{1}{l_{pb}} \tag{3}$$

where l_{tot} is the total mean free path. l_{pp}, l_{pd}, and l_{pb} are mean free paths produced by phonon–phonon interaction, phonon–defects interaction and phonon–boundary interaction, respectively. l_{pp} is related to intrinsic structure of composites and the most sensitive to temperature, while, l_{pd} and l_{pb} are related to the defects of composites.

Table 2
The values of A and B for the curve fitting in Fig. 3.

Samples	C/SiC	C/SiC–TaC-4	C/SiC–TaC-7	C/SiC–TaC-10
A ($\times 10^{-4}$ K^{-1} s/mm^2)	1.152	1.294	1.129	1.177
B ($\times 10^{-2}$ s/mm^2)	2.292	3.571	2.319	2.916

Parameter A represents the temperature dependent thermal diffusivity rate, which is determined by l_{pp}, thereby the intrinsic structure of the composites. As shown in Fig. 4, all the composites have the similar SiC matrix and PyC structure: PyC was covered by a continuous SiC that was formed in the RMI process; SiC and PyC were well bonded; and PyC showed a flake structure. The addition of TaC in C/SiC does not affect on the morphologies of the matrix and the reactions between silicon and carbon. All the composites have the same fiber preform, similar SiC matrix and PyC layer structure, which are the reasons for the close A values for all the composites, thereby the same temperature dependent thermal diffusivity behavior.

Parameter B is determined by l_{pd} and l_{pb}. It is therefore related to the defects of the composites. Fig. 5 shows typical defects in all of the four composites, including pores (Fig. 5a), grain boundary (Fig. 5b), interfaces and cracks (Fig. 5c). As indicated in Fig. 5b, there is little difference in the morphology of the formed SiC by RMI process.

Therefore, the contribution of phonon and grain boundary interaction should be considered the same for all the composites. C/SiC–TaC-7 has the lowest porosity among the composites with TaC addition, so that the interaction between phonons and holes is the weakest. The mean free path is thus the maximum and has a large thermal diffusivity and small B value. The mean free path for C/SiC is long because there is no PyC/TaC interface inside. The thermal diffusivity of C/SiC is thus high.

In the thermal diffusion curves (Fig. 3), there is a transition point (1200 °C), at which the temperature dependent thermal diffusivity rate is changed. Since all the composites have the same transition temperature, it is not caused by the addition of TaC into C/SiC. As aforementioned, the temperature dependent thermal diffusivity rate is determined by the intrinsic structure of the composites. It is believed that the transition point may be caused by the structural change at the temperature beyond 1200 °C. Such structural changes may occur in the process of testing, including the interface change, the phase transformation, and the phase redistribution. In order to fit the curves in Fig. 3 over the whole temperature range, we use a multinomial formula according to Ref. [25]. The correlation coefficients for such fittings are more than 0.98.

$$\alpha_{C/SiC} = -4.67 - \frac{8.49 \times 10^5}{T^{1.91\times10^4}} + 5.04 * \exp\left(\frac{26.1}{T^{0.5}}\right) \tag{4}$$

$$\alpha_{C/SiC-TaC-4} = -3.39 - \frac{26.99}{T^{3.15\times10^2}} + 3.99 * \exp\left(\frac{24.87}{T^{0.5}}\right) \tag{5}$$

$$\alpha_{C/SiC-TaC-7} = -3.31 + \frac{1312.07}{T^{8.77\times10^2}} + 4.64 * \exp\left(\frac{43.32}{T^{0.46}}\right) \tag{6}$$

$$\alpha_{C/SiC-TaC-10} = -4.62 + \frac{4.64 \times 10^8}{T^{1.98\times10^5}} + 4.7 * \exp\left(\frac{20.56}{T^{0.46}}\right) \tag{7}$$

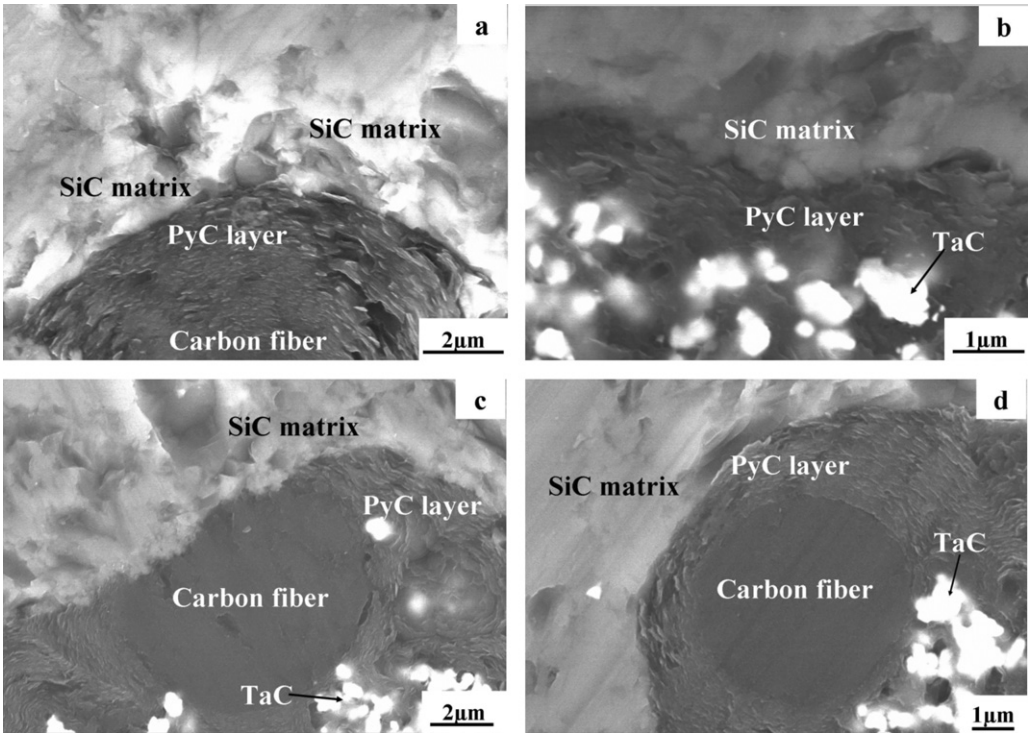

Fig. 4. Structures of the composites: (a) C/SiC; (b) C/SiC–TaC-4; (c) C/SiC–TaC-7; (d) C/SiC–TaC-10.

An exponential term is shown in the fitting equation. According to Ref. [25], it should correspond to a new mechanism that may lead to the transition of thermal diffusivity. In this study, the mechanism should be the structural change in composites at temperatures beyond 1200 °C. The exponential term is an energy term to make the transition happen. According to Arrhenius equation, the activation energies of these transitions are 8.33 kJ/mol, 7.94 kJ/mol, 7.71 kJ/mol, and 8.78 kJ/mol for C/SiC, C/SiC–TaC-4, C/SiC–TaC-7 and C/SiC–TaC-10, respectively. The smaller activation energy means that the transition more easily happens.

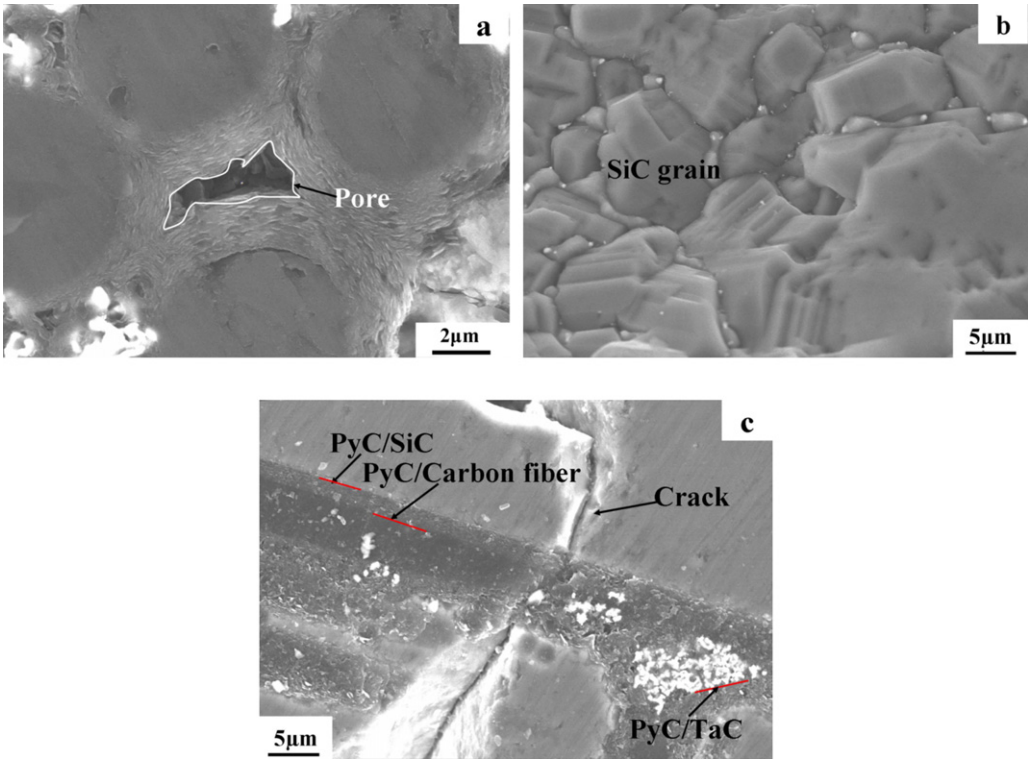

Fig. 5. Defects in the composites: (a) pore; (b) SiC grain boundary; (c) interfaces and cracks.

4. Conclusions

3D needled C/SiC–TaC composites were prepared by slurry infiltration combined with reactive melt infiltration. The effect of microstructure and composition of composites on the thermal diffusivity were investigated. A model considering lattice vibration and microstructure was used to explain thermal diffusivity of C/SiC–TaC composites. The results indicated that the temperature dependent thermal diffusivity rate did not change with the different TaC content. The thermal diffusivity values were influenced by microstructure: the fewer defects and boundaries, the higher values. The thermal diffusivity curves of the composites could be well fitted by a multinomial function, in which the exponential term led to a transition at 1200 °C. The transition of the thermal diffusivity is related to the structural change in the composites.

Acknowledgements

This work is financially supported by the Chinese Natural Science Foundation (Grant No. 90916030), the Research Fund of State Key Laboratory of Solidification Processing (NWPU) (Grant No. 21-TP2007), and "111" project (B08040).

References

[1] R. Naslain, A. Guette, F. Rebillat, R. Pailler, F. Langlais, X. Bourrat, Boron-bearing species in ceramic matrix composites for long-term aerospace applications, J. Solid State Chem. 177 (2004) 449–456.
[2] S. Schmidt, S. Beyer, H. Knabe, H. Immich, R. Meistring, A. Gessler, Advanced ceramic matrix composite materials for current and future propulsion technology applications, Acta Astron. 55 (2004) 409–420.
[3] T.M. Besmann, B.W. Sheldon, R.A. Lowden, D.P. Stinton, Vapor phase fabrication and properties of continuous filament ceramic composites, Science 253 (1991) 1104–1109.
[4] F. Christin, Design, fabrication, and application of thermostructural composites (TSC) like C/C, C/SiC, and SiC/SiC composites, Adv. Eng. Mater. 4 (2002) 903–912.
[5] W.G. Fahrenholtz, G.E. Hilmas, Future ultrahigh temperature materials. UHTM Workshop Draft Report NSF-AFOSR Joint Workshop on Future Ultra-High Temperature Materials (2004).
[6] Y.G. Wang, Q.M. Liu, J.L. Liu, L.T. Zhang, L.F. Cheng, Deposition mechanism for chemical vapor deposition of zirconium carbide coatings, J. Am. Ceram. Soc. 91 (2008) 1249–1252.
[7] H.B. Li, L.T. Zhang, L.F. Cheng, Y.G. Wang, Ablation resistance of different coating structures for C/ZrB_2–SiC composites under oxyacetylene torch flame, Int. J. Appl. Ceram. Technol. 6 (2009) 145–150.
[8] Y.G. Wang, W. Liu, L.F. Cheng, L.T. Zhang, Preparation and properties of 2D C/ZrB_2–SiC ultra high temperature ceramic composites, Mater. Sci. Eng. A 524 (2009) 129–133.
[9] H. Hu, Q. Wang, Z. Chen, C. Zhang, Y. Zhang, J. Wang, Preparation and characterization of C/SiC–ZrB_2 composites by precursor infiltration and pyrolysis process, Ceram. Int. 36 (2010) 1011–1016.
[10] H.B. Li, L.T. Zhang, L.F. Cheng, Y.G. Wang, Oxidation analysis of 2D C/ZrC–SiC composites with different coating structures in CH_4 combustion gas environment, Ceram. Int. 35 (2009) 2277–2282.
[11] Y. Wang, Y.D. Xu, Y.G. Wang, L.F. Cheng, L.T. Zhang, Effects of TaC addition on the ablation resistance of C/SiC, Mater. Lett. (2010) 2068–2071.
[12] Z. Chen, X. Xiong, G. Li, Y. Wang, Ablation behaviors of carbon/carbon composites with C-SiC–TaC multi-interlayers, Appl. Surf. Sci. (2009) 9217–9223.
[13] L. Li, Y.G. Wang, L.F. Cheng, L.T. Zhang, Preparation and properties of 2D C/SiC–ZrB_2–TaC composites, Ceram. Int. 37 (2011) 891–896.
[14] Y. Wang, X. Zhu, L. Zhang, L. Cheng, Reaction kinetics and ablation properties of C/C–ZrC composites fabricated by reactive melt infiltration, Ceram. Int. 37 (2011) 1277–1283.
[15] H. Tawil, L.D. Bentsen, S. Baskaran, D.P.H. Hasselman, Thermal diffusivity of chemically vapor deposited silicon carbide reinforced with silicon carbide or carbon fibers, J. Mater. Sci. 20 (1985) 3201–3212.
[16] R. Yamada, T. Taguchi, N. Igawa, Mechanical and thermal properties of 2D and 3D SiC/SiC composites, J. Nucl. Mater. 283–287 (2000) 574–578.
[17] R. Yamada, N. Igawa, T. Taguchi, S. Jitsukawa, Highly thermal conductive, sintered SiC fiber-reinforced 3D-SiC/SiC composites: experiments and finite-element analysis of the thermal diffusivity/conductivity, J. Nucl. Mater. 307–311 (2002) 1215–1220.
[18] S. Kumar, A. Kumar, A. Shukla, et al., Thermal-diffusivity measurement of 3D-stitched C–SiC composites, J. Euro. Ceram. Soc. 29 (2009) 489–495.
[19] F.H. Chung, Quantitative interpretation of X-ray diffraction patterns of mixtures. I. Matrix-flushing method for quantitative multicomponent analysis, J. Appl. Cryst. 7 (1974) 519–525.
[20] W.B. Hillig, Making ceramic composites by melt infiltration, Am. Ceram. Soc. Bull. 73 (1994) 56–62.
[21] R.J. Bruls, H.T. Hintzen, R. Metselaar, A new estimation method for the intrinsic thermal conductivity of nonmetallic compounds. a case study for $MgSiN_2$ AlN and Si_3N_4 Ceramics, J. Euro. Ceram. Soc. 25 (2005) 767–779.
[22] Z.D. Guan, Z.T. Zhang, J.S. Jao, Physical Performances of Inorganic Materials, Tsinghua University Press, Beijing, 1992, pp. 131–150.
[23] W.J. Parker, R.J. Jenkins, C.P. Butler, G.L. Abbott, Flash method of determining thermal diffusivity, heat capacity, and thermal conductivity, J. Appl. Phys. 32 (1961) 1679–1684.
[24] G. Amirthan, A.U. Kumar, M. Balasubramanian, Thermal conductivity studies on Si/SiC ceramic composites, Ceram. Inter. 37 (2011) 423–426.
[25] L.F. Cheng, Y.D. Xu, Q. Zhang, L.T. Zhang, Thermal diffusivity of 3D C/SiC composites from room temperature to 1400 °C, Carbon 41 (2003) 707–711.